ICSV13 - Vienna
The Thirteenth International Congress on Sound and Vibration
Vienna, Austria, July 2-6, 2006

VIBRATION ANALYSIS OF ROTATING MULTIDIRETIONAL LAMINATED COMPOSITE DISKS

Kyo-Nam Koo*

Department of Aerospace Engineering, University of Ulsan
San 29, Mugeo 2-dong, Nam-gu, Ulsan 680-749, Korea
knkoo@mail.ulsan.ac.kr

Abstract

Since fiber-reinforced composite materials has high specific strength and stiffness, an application of fiber reinforced composite materials to rotating disks can enhance the performance of machinery by increasing the dynamic stability and saving the driving energy. There have been few works on the vibration characteristics of rotating multidirectional laminated disks made of fiber-reinforced composite materials. Most of the previous researches have been confined to single lamina disks. When a disk rotates, the centrifugal force causes the in-plane loads that affect the vibration characteristics of rotating disk. In this paper, the exact expressions for the in-plane loads acting on rotating cross-ply laminate disk are presented. The vibration equation of rotating cross-ply laminate disk is solved by Galerkin's method. In the numerical examples, the natural frequencies and critical speeds of the rotating disks are discussed for various cross-ply ratios.

INTRODUCTION

Vibration of rotating disks is a major concern in data storage devices such as optical and magnetic disk drives as well as in industrial machines such as turbine rotors and circular saws, and so on. The demand for higher data transfer rate in computers causes a drastic increase of rotating speed in data storage disks. However, the rotating speed can be limited by the dynamic instability at the critical or flutter speeds.

As technology improvements in current optical and magnetic disk storage systems are saturating, Holographic Digital Data Storage (HDDS) is considered a promising technology that makes possible storage densities that exceed the barriers of traditional magnetic and optical recording [1]. In addition to some requirements for multiplexing method and storage material placed on the holographic media, the media must have dimensional and dynamic stability. Fiber reinforced composite materials have high specific modulus as well as very low coefficient of thermal expansion (CTE) in the fiber direction. The longitudinal CTE of some carbon/epoxy composite materials is negative. An application of fiber reinforced composite materials to data storage disks, especially to HDDS disk, in addition to rotating machinery, is expected to enhance both the vibration characteristics and the thermal stability.

The vibration analysis of rotating isotropic disks has attracted much attention since Lamb and Southwell [2] dealt with this problem. However, there are not many papers [3-7] on the vibration characteristics on rotating polar orthotropic disks. No work has been reported, to the author's best knowledge, on the vibration and critical speed of rotating laminated composite disks

In the present paper, the vibration analysis of rotating laminated composite disks is performed to calculate the natural frequencies and critical speeds. The closed-form solution for stress distribution of rotating laminated composite disk is found. Also, the dynamic equation of the disk is formulated. The approximate solution is obtained by Galerkin's method. Numerical results are given for Glass Fiber Reinforced Plastics (GFRP) cross-ply disks with a diameter of 120mm. The effect of cross-ply ratio on the natural frequencies and critical speeds is studied.

GOVERNING EQUATIONS AND SOLUTION METHOD

Constitutive Equation of Laminated Composite Disk

A composite laminate can be composed of as many layers as needed, of which fiber orientation could be arbitrary. One of the simple ways to make up a laminated composite disk is to stack the radially-reinforced and circumferentially-reinforced laminae as shown in Fig. 1. Laminates containing plies oriented only at 0° and 90° are called cross-ply laminates. The stress-strain relations for a layer in a laminated disk under plane stress are

$$\begin{Bmatrix} \sigma_1 \\ \sigma_2 \\ \tau_{12} \end{Bmatrix} = \begin{bmatrix} Q_{11} & Q_{12} & 0 \\ Q_{12} & Q_{22} & 0 \\ 0 & 0 & Q_{66} \end{bmatrix} \begin{Bmatrix} \varepsilon_1 \\ \varepsilon_2 \\ \gamma_{12} \end{Bmatrix} \text{ or } \boldsymbol{\sigma} = \mathbf{Q}\boldsymbol{\varepsilon} \tag{1}$$

where the subscripts 1 and 2 denote the fiber and transverse directions, respectively; $\mathbf{Q}$ is the reduced stiffness matrix [8].

Normally, the lamina principal axes (1, 2) do not coincide with the loading or reference axes. The stress-strain relations in Eq. (1) can be transformed into the disk body axes (r,θ) which is fixed at a disk as shown in Fig. 2:

$$\boldsymbol{\sigma}_{(r\theta)} = \overline{\mathbf{Q}}\boldsymbol{\varepsilon}_{(r\theta)} \tag{2}$$

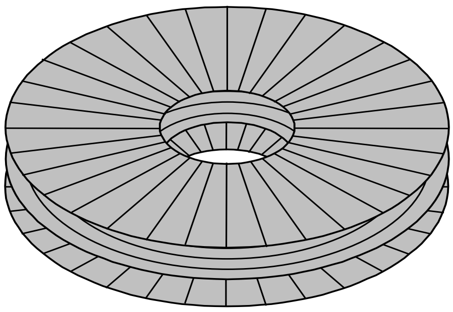

Fig. 1 - Laminated composite disk.

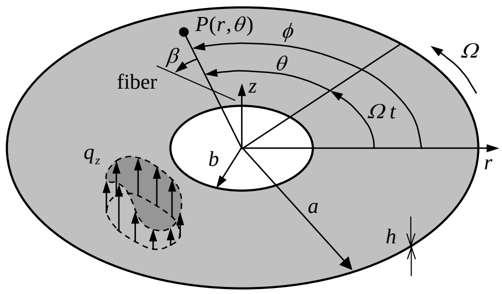

Fig. 2 - Coordinates and geometry of rotating disk.

where the reduce transformed matrix $\overline{\mathbf{Q}}$ is obtained by

$$\overline{\mathbf{Q}} = \mathbf{T}^{-1}\mathbf{Q}\mathbf{T}^{-\mathrm{T}} \tag{3}$$

where the transformation matrix $\mathbf{T}$ [8] is defined for the fiber orientation angle β measured positive counterclockwise from the r-axis as shown in Fig. 2.

The displacements of the disk in the coordinate (r,θ) can expressed by

$$u_r = u_r^0 - z\frac{\partial w}{\partial r}, \quad u_\theta = u_\theta^0 - z\frac{\partial w}{r\partial \theta}, \quad w = w \tag{4}$$

where the subscript 0 denotes the mid-plane.

The strain vector $\boldsymbol{\varepsilon}_{(r\theta)}$ in the polar coordinate are composed of the strain vector in the mid-plane $\boldsymbol{\varepsilon}^0_{(r\theta)}$ and the curvature vector $\boldsymbol{\kappa}_{(r\theta)}$:

$$\boldsymbol{\varepsilon}_{(r\theta)} = \boldsymbol{\varepsilon}^0_{(r\theta)} + z\boldsymbol{\kappa}_{(r\theta)} \tag{5}$$

Integrating Eq. (2) with the expression for strain in Eq. (5) gives the force resultants $\mathbf{N}_{(r\theta)}$, and integrating Eq. (2) multiplied by z yields the moment resultants $\mathbf{M}_{(r\theta)}$:

$$\mathbf{N}_{(r\theta)} = \mathbf{A}_{(r\theta)}\boldsymbol{\varepsilon}^0_{(r\theta)}, \quad \mathbf{M}_{(r\theta)} = \mathbf{D}_{(r\theta)}\boldsymbol{\kappa}_{(r\theta)} \tag{6}$$

where $\mathbf{A}_{(r\theta)}$ and $\mathbf{D}_{(r\theta)}$ are the extensional and bending stiffnesses, respectively, in the coordinate (r,θ); and their components can be defined as

$$A_{ij} = \int_{-h/2}^{h/2} \overline{Q}_{ij}\,dz, \quad D_{ij} = \int_{-h/2}^{h/2} \overline{Q}_{ij} z^2 dz. \tag{7}$$

Dynamic Equation of Motion

When a disk rotates in a constant speed Ω, the centrifugal force produces the in-plane force resultants $\overline{N}_r$ and $\overline{N}_\theta$. The dynamic equation of a rotating symmetric laminate disk in the coordinate (r,θ) may be expressed in the form

$$D_{rr}\left(\frac{\partial^4 w}{\partial r^4}+2\frac{\partial^3 w}{r\partial r^3}\right)+D_{\theta\theta}\left(\frac{\partial^4 w}{r^4\partial\theta^4}+2\frac{\partial^2 w}{r^4\partial\theta^2}-\frac{\partial^2 w}{r^2\partial r^2}+\frac{\partial w}{r^3\partial r}\right)$$
$$+2(D_{r\theta}+D_{ss})\left(\frac{\partial^4 w}{r^2\partial r^2\partial\theta^2}-\frac{\partial^3 w}{r^3\partial r\partial\theta^2}+\frac{\partial^2 w}{r^4\partial\theta^2}\right)-\frac{\partial}{r\partial r}\left(r\overline{N}_r\frac{\partial w}{\partial r}\right) \tag{8}$$
$$-\frac{\partial}{r\partial\theta}\left(\overline{N}_\theta\frac{\partial w}{\partial\theta}\right)+\rho h\frac{\partial^2 w}{\partial t^2}=q_z$$

where $w=w(r,\theta,t)$ is the transverse displacement of the point (r,θ) at time t; ρ is the density of the disk; $q_z=q_z(r,\theta,t)$ is the distributed load in z-direction.

The force resultants $\overline{N}_r$ and $\overline{N}_\theta$ in Eq. (8) are determined from the equilibrium equation in the r-direction:

$$-\frac{\partial}{\partial r}\left(r\overline{N}_r\right)-\frac{\partial\overline{N}_{r\theta}}{\partial\theta}+\overline{N}_\theta=\rho r^2\Omega^2 \tag{9}$$

With $\partial(\ )/\partial\theta=0$ for an axisymmetric situation, the force resultants may be derived from Eqs. (4) and (6):

$$\overline{N}_r=A_{rr}\frac{d\overline{u}_r}{dr}+A_{r\theta}\frac{\overline{u}_r}{r},\ \overline{N}_\theta=A_{r\theta}\frac{d\overline{u}_r}{dr}+A_{\theta\theta}\frac{\overline{u}_r}{r},\ \overline{N}_{r\theta}=A_{ss}\left(\frac{d\overline{u}_\theta}{dr}-\frac{\overline{u}_\theta}{r}\right) \tag{10}$$

Along with $\partial\overline{N}_{r\theta}/\partial\theta=0$, substituting the resultants in Eq. (10) into Eq. (9) yields the differential equation:

$$r^2\frac{d^2\overline{u}_r}{dr^2}+r\frac{d\overline{u}_r}{dr}-\mu^2\overline{u}_r=-\frac{\rho h\Omega^2 r^3}{A_{rr}} \tag{11}$$

where $\mu^2=A_{\theta\theta}/A_{rr}$. Since the solution of Eq. (11) depends on the value of μ^2, we should consider two cases: $\mu^2\neq 9$ and $\mu^2=9$.

The boundary conditions are expressed for a disk fixed at inner radius b and free at outer radius a as follows:

$$\bar{u}_r(b) = 0\,, \qquad \bar{N}_r(a) = 0 \tag{12}$$

The solution satisfying the boundary conditions is given by:

$$\bar{u}_r(r) = \frac{\rho h \Omega^2}{kA_{rr}} \frac{C_1 r^{\mu} + C_2 r^{-\mu} - r^3 g(r)}{(\mu+\nu)(a/b)^{\mu} + (\mu-\nu)(b/a)^{\mu}} \tag{13}$$

where

$$\nu = A_{r\theta} / A_{rr} \tag{14.a}$$

$$C_1 = \{\delta_{\mu 3} + (3+\nu) g(a)\} a^3 b^{-\mu} + (\mu - \nu) g(b) a^{-\mu} b^3 \tag{14.b}$$

$$C_2 = \{\delta_{\mu 3} + (\mu+\nu) g(a)\} a^{\mu} b^3 - (3+\nu) g(b) a^3 b^{\mu} \tag{14.c}$$

$$\begin{cases} k = 9 - \mu^2, \ \delta_{\mu 3} = 0, \ \ g(r) = 1 & \text{for } \mu \neq 3 \\ k = 6, \qquad \ \ \delta_{\mu 3} = 1, \ \ g(r) = \ln r & \text{for } \mu = 3 \end{cases} \tag{14.d}$$

Then, the force resultants necessary in Eq. (8) may be obtained by substituting Eq. (13) into Eq. (10).

Method of Solution

The eigensolutions of Eq. (14) for free vibration may be sought by assuming $q_z = 0$ and

$$w(r,\theta,t) = R(r)\cos(n\theta)e^{i\omega t} \tag{15}$$

Substituting Eq. (15) into Eq. (8) with $q_z = 0$ changes the partial differential equation into an ordinary differential equation, of which an approximate solution, then, is sought of the form:

$$R(r) = \sum_{k=1}^{N} q_k f(r)_k \tag{16}$$

Applying Galerkin's method, the coefficients q_k will be determined from the system of equations:

$$\int_b^a \left(\mathcal{L}[\sum_{k=1}^{N} q_k f_k] - \omega^2 \rho h \sum_{k=1}^{N} q_k f_k\right) f_l dr = 0 \tag{17}$$

where $\mathcal{L}$ is the linear operator for the ordinary differential equation.

The system of equations may be written in the matrix form:

$$(\mathbf{K}_b + \Omega^2\mathbf{K}_\Omega - \omega^2\mathbf{M})\mathbf{q} = \mathbf{0} \tag{18}$$

where $\mathbf{K}_b$ is the stiffness matrix due to bending; $\mathbf{K}_\Omega$ is the stiffness matrix including a gyroscopic effect; $\mathbf{M}$ is the mass matrix.

The ground-based observer sees two different natural frequencies of single mode known as a mode splitting. Those are the forward and backward frequencies, ω^f and ω^b given by

$$\omega^f = \omega + n\Omega, \quad \omega^b = \omega - n\Omega. \tag{19}$$

The critical speed can be determined when the backward frequency ω^b vanishes. At this situation, the propagation speed of a backward traveling wave in the rotating frame is equal to the disk rotation speed.

The accuracy of the solution of Eq. (18) depends on the choice of the functions $f_i(r)$. The orthogonal polynomial functions proposed by Bhat [9] will be used to have a stable solution. Koo [7] successfully applied these functions to the lateral vibration of rotating polar orthotropic disks.

RESULTS

The rotating disks are assumed to have the same dimensions as those of typical optical storage media with b = 15 mm, a = 60 mm, h = 1.2 mm. To study the effect of the material property on the natural frequencies and critical speeds of the rotating disks, a typical GFRP(E-glass/Epoxy) is chosen and its material properties are given by

$$E_1 = 38.6\text{GPa},\ E_2 = 8.27,\ G_{12} = 4.14,\ \nu_{12} = 0.26,\ \rho = 1800\ \text{kg/m}^3$$

Since a single lamina disk of orthotropic material may fail in matrix at a low level of stress or impact, a multidirectional laminated disk can be a more practical design. While $[0/90]_S$ and $[90/0]_S$ disks have the same A_{ij}'s, their D_{ij}'s are different. The natural frequencies of the $[0/90]_S$ and $[90/0]_S$ disks are obtained at various rotating speeds from which critical speeds are determined.

The frequency-speed diagram of the $[0/90]_S$ disk is shown in Fig. 3 and that of the $[90/0]_S$ disk in Fig. 4. The lowest six modes of the disks in non-rotating do not have a nodal circle. A close examination reveals that the natural frequencies of the $[0/90]_S$ disk are higher in modes (0,0) to (0,2) and are lower in modes (0,3) to (0,5) than those of the $[90/0]_S$ disk when the disks are not rotating. This is because D_{rr} is higher than $D_{\theta\theta}$ in the $[0/90]_S$ disk, and vice versa in the $[90/0]_S$ disk. It can be said that the lower three modes are affected by the magnitude of D_{rr} whereas the higher three modes are dependent on the value of $D_{\theta\theta}$. The lowest critical speed of the $[0/90]_S$ disk is around

15,293 RPM in mode (0,3) while the second one is around 16,979 in mode (0,2). The lowest critical speed of the $[90/0]_S$ disk is around 14,975 RPM in mode (0,2) like the polycarbonate disk. This can be explained by the relationship between the natural frequency and bending stiffness.

To study the effect of the amount of 0° layers on the critical speed of cross-ply laminate disk, the cross-ply ratio is defined as

$$M = \frac{i}{j} \tag{20}$$

where i and j are the total thickness of 0° and 90° layers, respectively; they become the number of the layers if all the layers have an equal thickness. The cross-ply laminate disks studied in this paper have a stacking sequence $[0_i/90_j]_S$ and $[90_i/0_j]_S$ where i and j are the integer numbers from 0 to 10 with $i + j = 10$, keeping the disk

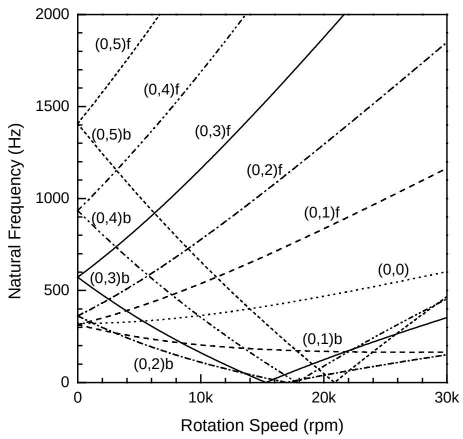

Fig. 3 - Frequency-speed diagram for $[0/90]_S$ disk.

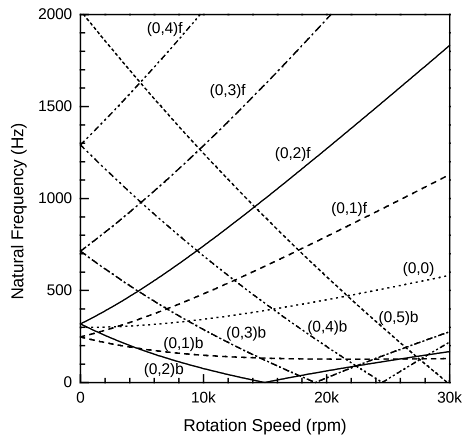

Fig. 4 - Frequency-speed diagram for $[90/0]_S$ disk.

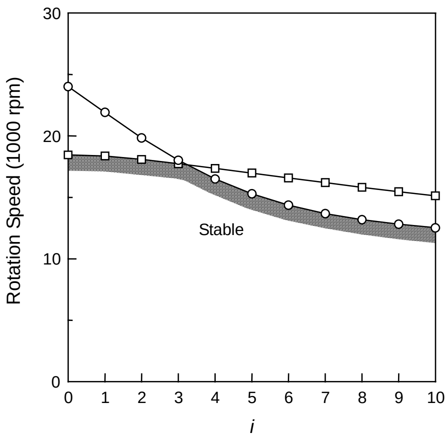

Fig. 5 - Critical speeds of $[0_i/90_{10-i}]_S$ disk. □ mode (0,2); ○ mode (0,3).

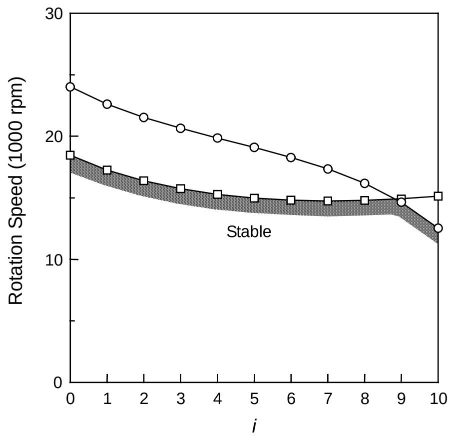

Fig. 6 - Critical speeds of $[90_i/0_{10-i}]_S$ disk. □ mode (0,2); ○ mode (0,3).

thickness h to 1.2 mm.

The lowest critical modes of the $[0_i/90_{10-i}]_S$ disks occur in mode (0,2) for $i \le 3$ and in mode (0,3) for $i \ge 4$ as shown in Fig. 5. This result is due to the fact that D_{rr} is greater than $D_{\theta\theta}$ near $i = 2$. Fig. 6 illustrates the lowest critical modes of the $[90_i/0_{10-i}]_S$ GFRP disks which are modes (0,2) for $i \le 8$ and mode (0,3) for $i \ge 9$. The same explanation can be applied to this phenomenon.

CONCLUSIONS

In the present paper, the vibration analysis of rotating laminated composite disks is performed to calculate the natural frequency and critical speed. The closed-form solution for the stress distribution of rotating laminated composite disk is found. Dynamic equation of rotating laminated composite disk is formulated. The approximate solution is obtained by Galerkin's method.

The numerical results show that the critical speeds of the laminated composite disk are strongly dependant on the ratio of the bending stiffnesses in radial and circumferential directions. Especially, for the cross-ply laminate disks, the $[0_i/90_j]_S$ disks have higher critical speeds at the cross-ply ratio less than one whereas the $[90_i/0_j]_S$ disks are more stable over the cross-ply ratio of one.

REFERENCES

[1] http://www.inphase-technologies.com/technology/whitepapers/index.html

[2] Lamb H., Southwell R.V., "The vibration of a spinning disk," *Proceedings of the Royal Society*, **99**, 272-280 (1921).

[3] Ghosh N.C., "Thermal effect on the transverse vibration of high speed rotating anisotropic disk," *Journal of Applied Mechanics*, **52**, 543-548 (1985).

[4] Son H., Kikuchi N., Ulsoy A.G., Yigit A.S., "Dynamics of prestressed rotating anisotropic plates subject to transverse loads and heat sources, part I: modelling and solution method," *Journal of Sound and Vibration*, **236**, 457-485 (2000).

[5] Son H., Kikuchi N., Ulsoy A.G., Yigit A.S., "Dynamics of prestressed rotating anisotropic plates subject to transverse loads and heat sources, part II: application to a specially orthotropic disk," *Journal of Sound and Vibration*, **236**, 457-485 (2000).

[6] Liang D.-S., Wang H.-J., Chen L.-W., "Vibration and stability of rotating polar orthotropic annular disks subjected to a stationary concentrated transverse load," *Journal of Sound and Vibration*, **250**, 795-811 (2002).

[7] Koo K.-N., "Vibration analysis and critical speeds of polar orthotropic annular disks in rotation," *Composite Structures*, The Special Issue for ICCM 15, (Accepted).

[8] Jones R.M., *Mechanics of Composite Materials*. (McGraw-Hill, New York, 1975)

[9] Bhat B.-H., "Natural frequencies of rectangular plates using characteristic orthogonal polynomials in Rayleigh-Ritz method," *Journal of Sound and Vibration*, **102**, 493-499 (1985).